In: Advances in Boundary Element Techniques VII, edited by B.Gatmiri, A.Sellier, M.H.Aliabadi,
Published by EC Ltd., Eastleigh, UK, 2006, ISBN: 0-9547783-3-2, p.15-22

Numerical Solution of a Free-Boundary Problem for Percussive Deep Drilling Modeling by BEM

S.E. Mikhailov[1] and I.V.Namestnikova[2]

[1,2]Div. of Mathematics, Glasgow Caledonian Univ., Cowcaddens Road, Glasgow, G4 0BA, UK,
s.mikhailov@gcal.ac.uk, i.namestnikova@gcal.ac.uk

Keywords: elasticity, boundary rupture, free-boundary problem, contact problem, iterative algorithm

Abstract. A numerical technique related to a stationary-periodic quasi-static model of rock percussive deep drilling is presented. The rock is modeled by an infinite elastic space with a semi-infinite circular cylindrical bore-hole having a curvilinear bottom. An auxiliary problem of stationary indentation of a rigid drill bit is considered first, where it is assumed that the indentation is produced by a stationary motion of the rupture front on which an appropriate rock strength condition is violated. The bore-hole boundary is not known in advance and consists of four parts: a traction-free non-rupturing part, a contact non-rupturing part, a traction-free part of the rupture front, and a contact part of the rupture front. Thus the problem is formulated as a non-classical non-linear free-boundary contact problem of elasticity. A multi-stage hierarchical iterative algorithm is implemented reducing the problem to a sequence of mixed problems of linear elasticity with known non-smooth infinite boundaries. The Boundary Element Method is used on each iteration step for numerical solution of the direct boundary integral equations of the axially-symmetric linear elastic problems. Then the stationary-periodic percussive drilling problem is reduced to the stationary problem on the rupture stage of the cycle and to the classical contact problem on the reverse and progression-before-rupture stages of the cycle. A numerical example of the stress and displacement distributions, and progression-force diagram are presented.

General Model Description

The drill-bit progression in the percussive drilling is caused by a material rupture under the action of the bit applied at the bore-hole boundary points $x(t)$ moving in time t due to rupture. This boundary loading generates stress $\sigma_{ij}(x,t)$ and strain $\varepsilon_{ij}(x,t)$ tensors at all material points x. Let a material point x has Cartesian coordinates (x_1, x_2, x_3) in the non-deformed state. The radius-vector of the same material point x in a deformed state at a time t is $\tilde{x}(x,t) = x + u(x,t)$, where $u(x,t)$ is the displacement vector. We will use all equations in terms the non-deformed (reference) coordinates x and refer the boundary conditions to the non-deformed boundary surfaces (the Lagrange approach).

Let us consider stationary-periodic percussive drilling of a half-infinite bore-hole, $\Omega_H(t)$, spreading to $x_3 = \infty$ in an infinite elastic space, see Fig. 1. Let the x_3-axis of the coordinate system coincide with the bore-hole axes, and the drill bit progressive-periodic motion occurs only in the x_3 direction. Let $\Omega(t) = \mathbb{R}^3 \backslash \Omega_H(t)$ be the domain occupied by the material (i.e. the infinite space with a drilled out bore-hole) and $\partial\Omega(t)$ be the bore-hole surface in the non-deformed state, while $\tilde{\Omega}_H(t)$, $\tilde{\Omega}(t) = \mathbb{R}^3 \backslash \tilde{\Omega}_H(t)$ and $\partial\tilde{\Omega}(t)$ be their counterparts in the deformed state. If the rupture front $\partial_F\Omega(t)$ constitutes only a finite part of the boundary $\partial\Omega(t)$, then the borehole is a semi–infinite cylinder with a curvilinear bottom being the rupture front $\partial_F\Omega(t)$. Otherwise, the bore-hole has a monotonously widening shape. If the bit is axially-symmetric then the bore-hole is axially symmetric as well. Let $B(t)$ be the domain occupied by the bit at an instant t, and $\partial B(t)$ be its surface.

To describe the material strength of a point x, we will use an instant strength condition at a point x at an instant t written as

$$\Lambda(\sigma(x,t)) < 1, \quad x \in \Omega(t), \tag{1}$$

where the function $\Lambda(\sigma)$ is associated with the von Mises (see expression (25)), Coulomb–Mohr, Drucker–Prager or another appropriate strength condition. We suppose that the rupture appears in

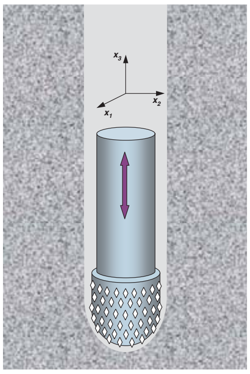

Figure 1: Stationary-periodic percussive drilling model

the form of a rupture front $\partial_F\Omega(t)$, which is a part of the bore-hole boundary $\partial\Omega(t)$. The rupture front equation can be taken as

$$\Lambda(\sigma(x), t) = 1, \quad y \in \partial_F\Omega(t), \tag{2}$$

while no rupture will be inside the material domain Ω and on the rest of the boundary, $\partial_V\Omega(t)$,

$$\Lambda(\sigma(x), t) < 1, \quad y \in \partial_V\Omega(t). \tag{3}$$

The simplest model can be obtained under the following

Model assumptions:

(i) The deformation gradient is small.

(ii) The drilled material is linearly elastic and homogeneous, i.e. its elastic moduli $C_{ijkl} = const$.

(iii) The bit is rigid.

(iv) The borehole surface is loaded by the bit at the contact surfaces and is free of tractions at all other points.

(v) Friction between bit and rock can be neglected.

(vi) The ruptured material, for which strength condition (1) is not satisfied, disappears (is washed away) thus leaving the fresh rupture front (the bottom of the bore-hole) either free of tractions or in contact with the bit bottom.

Under the model assumptions, the non-rupturing boundary part $\partial_V\Omega(t)$ generally consists of the traction-free non-rupturing part, $\partial_{0V}\Omega(t)$, and a contact non-rupturing part, $\partial_{cV}\Omega(t)$. Similarly, the rupturing boundary part $\partial_F\Omega(t)$ generally consists of a traction-free rupturing part, $\partial_{0F}\Omega(t)$, and a contact rupturing part, $\partial_{cV}\Omega(t)$.

Stationary Indentation Model

Let us consider in this section an auxiliary problem of stationary indentation of an infinite elastic space by a rigid indentor (bit) with an instant bit progression $h_3(t)$ (the lowest x_3 coordinate of the bit boundary) in the x_3 direction, where $h_3(t) < 0$ and $h(t) = (0, 0, h_3(t))$ is the indentor progression vector.

Let $\eta_j(x)$ be a unit outward (i.e. directed inward the bore-hole) normal vector to the *non-deformed* boundary $\partial\Omega(t)$. As shown in [1], the non-rupturing boundary part $\partial_V\Omega(t)$ consists of cylindrical pieces with the vertical axis parallel to the progression vector h, i.e.,

$$\eta_3(x) = 0, \quad x \in \partial_V\Omega(t), \tag{4}$$

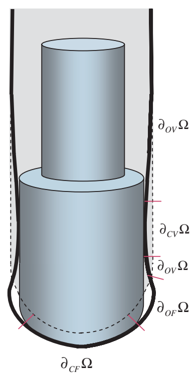

Figure 2: Bore-hole boundary partition

while on the rupturing part of the boundary,

$$\eta_i(x) > 0, \quad x \in \partial_F\Omega(t). \tag{5}$$

The boundary relations (4) and (5) mean that *there is no rupture on the cylindrical part of* $\partial\Omega$*, any non-cylindrical part of the boundary must be a rupture front and, moreover, there can be no material above the rupture front (in the non-deformed state).*

Summarising conditions (2), (3), (4) and (5), we can formulate them as unilateral nonlinear boundary conditions on the whole boundary,

$$\Lambda(\sigma(x)) - 1 \leq 0, \tag{6}$$

$$\eta_3(x) \geq 0, \tag{7}$$

$$(\Lambda(\sigma(x)) - 1)\eta_3(x) = 0, \quad x \in \partial\Omega. \tag{8}$$

Another set of nonlinear boundary conditions is given by unilateral contact conditions that can be written as a (slightly generalised) Signorini's problem , cf. [2, 3, 4],

$$d'(\tilde{x}) \geq 0, \tag{9}$$

$$\sigma_{ij}(x)\eta_j(x)\eta_i(x) \leq 0, \tag{10}$$

$$d'(\tilde{x})\sigma_{ij}(x)\eta_j(x)\eta_i(x) = 0, \quad x \in \partial\Omega, \tag{11}$$

where

$$d'(\tilde{x}) := (x_i^B(\tilde{x}) - \tilde{x}_i)\eta'_i(x)$$

is a (positive or negative) distance between the point $\tilde{x}$ and the bit boundary ∂B in the $\eta'(x)$ direction; the distance is taken positive, when the point $\tilde{x}$ in the deformed state is outside B and negative, when it is inside; $\eta'_i(x)$ is a unit vector making a sharp (or zero) angle with the external normal $\tilde{\eta}_i(x)$ to $\partial\Omega$ and can be chosen as convenient for particular applications, e.g., as $\eta_i(x)$ or $\tilde{\eta}_i(x)$; and $x_i^B(\tilde{x})$ is a point on ∂B such that the vector $x_i^B(\tilde{x}) - \tilde{x}$ lies along $\eta'_i(x)$.

The strict inequality in (9) and equality in (10) are satisfied at points on the traction-free boundary $\partial_0\Omega$ consisting of $\partial_{0V}\Omega$, $\partial_{0F}\Omega$ and a junction curve between them, while the equality in (9) and strict inequality in (10) are satisfied at points on the contact boundary $\partial_c\Omega$ consisting of $\partial_{cV}\Omega$, $\partial_{cF}\Omega$ and a junction curve between them.

Note that if the displacements $u(x)$ are small, boundary condition (9) can be linearised as

$$u_i(x)\eta'_i(x) \leq d(x), \quad x \in \partial\Omega, \tag{12}$$

where $d(x) = (x_i^B(x) - x_i)\eta'_i(x)$ is a (positive or negative) distance between the point x and the bit boundary ∂B in the $\eta'(x)$ direction in the non-deformed state, and it is known if the contact surface is known and is to be determined otherwise.

To solve the stationary indentation problem, it is sufficient to consider it only for $t = 0$. Thus, taking into account relations (6)-(9) and dropping the argument $t = 0$ for brevity, we arrive at the following non-classical non-linear free boundary problem,

$$\sigma_{ij,j}(x) = 0, \qquad \Lambda(\sigma(x)) < 1, \qquad x \in \Omega; \tag{13}$$

$$\begin{array}{llll} \sigma_{ij}(x)\eta_j(x)\xi_i(x) = 0, & \sigma_{ij}(x)\eta_j(x)\zeta_i(x) = 0, & \sigma_{ij}(x)\eta_j(x)\eta_i(x) < 0, & \\ \eta_3(x) = 0, & d'(x+u(x)) = 0, & \Lambda(\sigma(x)) < 1, & x \in \partial_{cV}\Omega; \end{array} \tag{14}$$

$$\begin{array}{llll} \sigma_{ij}(x)\eta_j(x)\xi_i(x) = 0, & \sigma_{ij}(x)\eta_j(x)\zeta_i(x) = 0, & \sigma_{ij}(x)\eta_j(x)\eta_i(x) < 0, & \\ \eta_3(x) > 0, & d'(x+u(x)) = 0, & \Lambda(\sigma(x)) = 1, & x \in \partial_{cF}\Omega; \end{array} \tag{15}$$

$$\begin{array}{llll} & \sigma_{ij}(x)\eta_j(x) = 0, & & \\ \eta_3(x) = 0, & d'(x+u(x)) > 0, & \Lambda(\sigma(x)) < 1, & x \in \partial_{0V}\Omega; \end{array} \tag{16}$$

$$\begin{array}{llll} & \sigma_{ij}(x)\eta_j(x) = 0, & & \\ \eta_3(x) > 0, & d'(x+u(x)) > 0, & \Lambda(\sigma(x)) = 1, & x \in \partial_{0F}\Omega; \end{array} \tag{17}$$

$$u_i(x) \to 0, \qquad x \to \infty. \tag{18}$$

Here

$$\sigma_{ij}(x) = \sigma^0_{ij} + C_{ijkl}\varepsilon_{kl}(x), \quad \varepsilon_{kl}(x) = (u_{k,l} + u_{l,k})/2, \tag{19}$$

and the constant stiffness tensor C_{ijkl} and the constant *in situ* stress σ^0_{ij} in the rock without the drill hole are know; $\xi_j(x)$, $\zeta_j(x)$ are unit vectors orthogonal to the normal vector $\eta_j(x)$ and to each other. Condition (18) is understood on almost any straight ray originating from $x = 0$, thus permitting a non-zero limit of the displacements as $x \to \infty$ parallel to the bore-hole.

All the four boundary parts $\partial_{0V}\Omega$, $\partial_{0F}\Omega$, $\partial_{cV}\Omega$, $\partial_{cF}\Omega$, and consequently $d'(x)$, are generally unknown in this setting, and the corresponding "excessive" boundary equalities and inequalities are provided in (14)-(17) to allow their determination.

After solving problem (13)-(19), the integration of the component $\sigma_{3j}(x)\eta_j(x)$ of the contact traction gives the total axial force $P(t)$ applied to the bit during the progression,

$$\mathcal{P}(t) = \int_{\partial_c\Omega} \sigma_{3j}(x)\eta_j(x)\, dS(x_c). \tag{20}$$

Stationary-Periodic Indentation Model

To model the stationary-periodic motion of the drill-bit, in addition to the Model assumptions (i)-(vi), let as make the following

Reverse assumption:

(vii) The rupture does not proceed during the reverse stage of the bit motion, i.e. the borehole boundary consists of the same material points until the load reaches the extremum value during the next cycle.

Due to assumption (vii), the stress and strain return to the same states during the reverse and the following progressive stages of the bit motion up to the rupture restarts. This implies the reverse and the following progressive stages can be considered as some interruptions of the stationary progression process, analyzed in the previous section, and moreover, the interruptions do not influence the material rupture. This means the relation between the total force and the bit progression looks as on Fig. 3, that is the elastic loading stage is followed by the rupture stage followed by the elastic unloading stage. Generally the elastic stages are non-linear on the loading and unloading stages due to the changing contact surface between the bit and the drilled material, and the force is constant on the rupture stage. The extremum force and strains in the process coincide with those obtained in the stationary indentation analysis in the previous section.

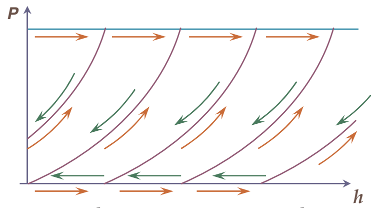

Figure 3: $h - P$ diagram in the stationary-periodic instant rupture model.

Then solution of the stationary indentation problem from the previous section fixes the bore-hole boundary for the reverse stage and gives the extremum values of the contact distribution $p(x, t^{ex})$, whose integral (20) gives the maximum force $\mathcal{P}^{ex} = \mathcal{P}(t^{ex})$ on the bit.

To predict the curvilinear part of the $h - P$ diagram, one has to solve the conforming linearly elastic contact problem with a material boundary $\partial\Omega$ known in the non-deformed state, for both the progressive (before rupture restart) and reverse stages of the cycle (which do coincide). The problem consists of the following equations,

$$\sigma_{ij,j}(x) = 0, \qquad x \in \Omega; \tag{21}$$

$$\begin{aligned} \sigma_{ij}(x)\eta_j(x)\xi_i(x) &= 0, & \sigma_{ij}(x)\eta_j(x)\zeta_i(x) &= 0, & & \\ u_i(x)\eta_i(x) &= d(x, h_3), & \sigma_{ij}(x)\eta_j(x)\eta_i(x) &< 0, & x &\in \partial_c\Omega(h_3); \end{aligned} \tag{22}$$

$$\sigma_{ij}(x)\eta_j(x) = 0, \qquad u_i(x)\eta_i(x) < d(x, h_3), \qquad x \in \partial_0\Omega(h_3); \tag{23}$$

$$u_i(x) \to 0, \qquad x \to \infty. \tag{24}$$

The overall boundary $\partial\Omega$ here is known from the end of the previous progression-rupture stage, although the boundary partition into the traction-free and contact parts is to be determined for each h_3.

Classical conforming contact problem (21)-(24), (19) can be solved by any of the well known methods, see e.g. [3]. Particularly, one can use the iteration algorithm similar to the one on the progression-rupture stage described above, that is, to choose some reasonable partition of $\partial\Omega$ onto $\partial_0\Omega$ and $\partial_c\Omega$, solve mixed elasticity problem (21)-(24), (19), modify the partition of $\partial\Omega$ to alleviate the violation of inequalities in (22)-(24) and start the next iteration.

Numerics

Numerical Algorithm. Different strategies can be chosen to solve this problem, see e.g. [5], [6, Section 8], [3]. One of the possibilities is the iteration algorithm described below.

The algorithm to solve the stationary indentation (active loading) part of the cycle generally consists of iterations, each solving a non-linear (due to Λ) mixed boundary value problem (13)-(18), (19), where the inequalities are ignored, with some *fixed* boundaries, $\partial_{0V}\Omega$, $\partial_{0F}\Omega$, $\partial_{cV}\Omega$, $\partial_{cF}\Omega$, and consequently $d(x)$. The non-linear (due to Λ) mixed boundary value problem is in tern reduced to a sequence of linear mixed problems solved by BEM or FEM. Then the inequalities in (13)-(17) are checked and the boundaries are changed to alleviate the violation of inequalities, and the next iteration starts. Some more details of the algorithm are given below.

On the first iteration one can reasonably assume that the rupture front coincides with the contact part of the bit, $\partial_c B$, which in turn coincides with the bit bottom, $\partial_b B$, (consisting of the bit surface points with algebraically smallest x_3 coordinate, over the points with the same (x_1, x_2) coordinates), i.e. $\partial_{cF}\Omega = \partial_c B = \partial_b B$, $\partial_{0F}\Omega = \emptyset$, and there is no contact without rupture, i.e. $\partial_{cV}\Omega = \emptyset$. Those assumptions imply that the borehole free boundary $\partial_V\Omega$ is the semi-infinite cylindrical surface ended by the bit bottom, on the first iteration. Then the algorithm can presented as a following (inside-out) sequence of imbedded iterative process.

Active loading iteration algorithm:

(i) Solving mixed problems of linear elasticity for a homogeneous medium with prescribed boundary tractions on $\partial\Omega\backslash\partial_{cV}\Omega$, and zero shear tractions and prescribed normal displacements on $\partial_{cV}\Omega$, by a BEM/FEM code.

(ii) Iterative algorithm of the form $\sigma_{\eta\eta}^{(i)} = f(\sigma^{(i-1)}, \Lambda^{(i-1)})$ to satisfy the nonlinear boundary condition $\Lambda = 1$ on $\partial_{cF}\Omega$.

(iii) Iterative alternating algorithm to satisfy the contact conditions and determine the contact rupture-free part of the boundary, $\partial_{cV}\Omega$.

(iv) Iterative algorithm to determine the non-deformed contact rupture boundary, $\partial_{cF}\Omega$, of the borehole $\partial\Omega$, using the known bit boundary and and the material boundary displacements from previous iteration step.

(v) Iterative algorithm to determine the non-contact rupture front boundary, $\partial_{0F}\Omega$, excluding material at the zones where $\Lambda > 1$ and adding material to the non-contact rupture front boundary $\partial_{0F}\Omega$ where $\Lambda < 1$, at the previous iteration step.

After solving the active loading problem, the computation of the unloading part of the percussive drilling cycle includes only one iteration process,

(vi) Iterative alternating algorithm to solve the conforming contact problem for the unloading and non-active loading stages.

Axially Symmetric BEM. In numerical applications we considered the case of axially-symmetric drilling bit, and the mixed problems of linear elasticity lying in the foundation of our multi-stage iteration algorithm were reduced to corresponding axially symmetric direct boundary integral equation (BIE), see e.g. [7], on a semi-infinite (in the axially-symmetric setting) boundary of the bore-hole. The boundary element method with linear boundary elements has been used for numerical solution of the BIE. The boundary element mesh was uniform on the curvilinear part of the bore-hole and the adjacent vertical part of the boundary of approximately the same length, then the element size increased and the mesh ended with a semi-infinite boundary element. Tractions and displacements have been linearly approximated over all boundary elements except the semi-infinite one and the finite-length boundary element adjacent to it, where special approximations based on the known asymptotics of the solution and BIE kernel at infinity have been employed.

Numerical Example. In the numerical example presented in Fig. 4, 5, 6, the Von Mises strength condition was used, giving the following expression for Λ,

$$\Lambda(\sigma) = \frac{\sqrt{3\sigma_{ij}\sigma_{ij} - \sigma_{ii}\sigma_{jj}}}{\sqrt{2}\ \sigma_c} = \frac{\sqrt{(\sigma_1 - \sigma_2)^2 + (\sigma_2 - \sigma_3)^2 + (\sigma_3 - \sigma_1)^2}}{\sqrt{2}\ \sigma_c}, \tag{25}$$

where σ_c is the material strength under uniaxial loading. The Young modulus to strength ratio, $E/\sigma_c = 200$, and the Poisson ration, $\nu = 0.25$, were used in the calculations, cf. [8]. The *in situ* stress has been neglected, $\sigma^0_{ij} = 0$. The drill-bit with the spherical contact part of a radius R has been analysed.

Fig. 4 shows the numerical $h - P$ diagram, One can see that after about 20% nonlinear growth, the force increases virtually linear with the bit progression. Fig. 5 and Fig. 6 present distributions

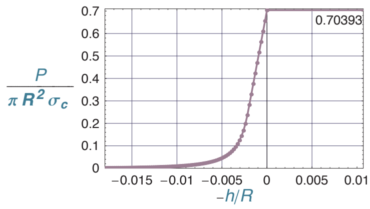

Figure 4: Numerical $h - P$ diagram for spherical bit and linearly elastic rock

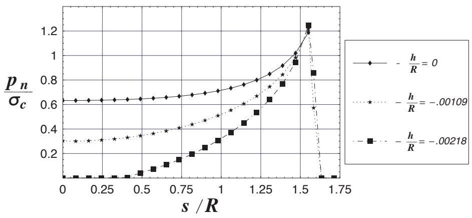

Figure 5: Boundary pressure distribution vs. arc length s

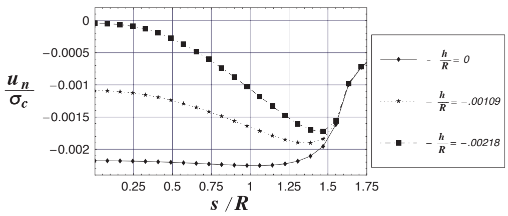

Figure 6: Boundary normal displacement distribution vs. arc length s

of the normal pressure and displacement, respectively, along the bottom of the bore-hole verses the boundary arc-length, at different values of bit progression.

In the performed calculations, we followed the multi-stage iteration algorithm described above, except item (v). This led to material overload ($\Lambda_{max} = 1.04$) on small $0.05R \times 0.07R$ zone adjacent to the upper end of the contact rupture front $\partial_{cF}\Omega$. This overload appearing in internal material points may be disregarded since the effective strength there is higher than in the contact boundary points due to action of the bit inserts on the boundary implicitly taken into account by this way.

Conclusions

A stationary-periodic quasi-static model of percussive drilling and an example of its numerical realisation are presented. The cycles of the bit progression – force diagram consist of three stages: elastic loading, constant-force rupture progression, and elastic unloading parallel to the loading. The problem is split into a stationary free-boundary non-linear problem for the rupture stage of the cycle, and a classical contact problem for the rest of the cycle. A multi-stage iteration algorithm is described reducing the solution to a sequence of linear mixed problems of elasticity. These linear problems can be solved by a general numerical method, e.g. the FEM or the Boundary Integral Equation Method. The latter method has been numerically implemented. As a result, this provides a nonlinear progression-force diagram, which is to be used in the bit dynamic motion prediction.

To take into account the damage zone, propagating ahead of the rupture zone, the rock material can be modeled as an elastic continuum with damage, decreasing the rock stiffness in the damage zone [9]. Extending the iterative algorithm, with an iterative stage taking into account damage, this non-linear problem is also reduced to a sequence of linear elastic problems solvable by the Boundary Integral Equation Method [10].

Acknowledgement. This work was supported by the research grant GR/R85556/01 "Nonlinear Dynamics and Rock Contact Fracture Mechanics in Modelling of Vibration Enhanced Drilling" of the Engineering and Physical Sciences Research Council, UK.

References

[1] S. E. Mikhailov and I. V. Namestnikova, Quasi-static stationary-periodic model of percussive deep drilling. In: *Proceedings of the 11th International Conf. on Computer Methods and Advances in Geomechanics* (G. Barla and M. Barla, eds.), Vol. 1, 103–109, Bologna: Patron Editore (2005).

[2] G. Duvaut and J. Lions, *Inequalities in Mechanics and Physics*, Berlin: Springer (1976).

[3] K. Johnson, *Contact Mechanics*, Cambridge: Cambridge University Press (1985).

[4] P. Wriggers, *Computational Contact Mechanics*, Chichester: John Wiley (2002).

[5] C. Eliot and J. Ockendon, *Weak and Variational Methods for Moving Boundary Problems*, Boston-London-Melbourne: Pitman (1982).

[6] J. Crank, *Free and Moving Boundary Problems*, Oxford (UK): Oxford University Press (1984).

[7] J. Balaš, J. Sladek and V. Sladek, *Stress Analysis by Boundary Element Methods*, Amsterdam-Oxford-New York-Tokyo: Elsevier (1989).

[8] R.D.Lama and V.S.Vutukuri, *Hanbook on Mechanical Properties of Rocks – Testing Techniques and Results*, Vol. 2, Clausthal (Germany): Trans Tech Publications (1978).

[9] S. E. Mikhailov and I. V. Namestnikova, Application of damage mechanics in percussive drilling modelling, in: *11th International Conf. on Fracture*, 8p., Turin, Italy, March 20-25 (2005).

[10] S. E. Mikhailov, Boundary-domain integro-differential equation of elastic damage mechanics model of stationary drilling, in: *Advances in Boundary Element Techniques VI* (A. P. S. Selvadurai, C. L. Tan and M. H. Aliabadi, eds.), 107–114, Eastligh, UK: EC Ltd. (2005).